

1 Prediction of outlet dissolved oxygen in micro-irrigation sand media 2 filters using a Gaussian process regression

3 Paulino J. García-Nieto^{a,*}, Esperanza García-Gonzalo^a, Jaume Puig-Bargués^b, Miquel
4 Duran-Ros^b, Francisco Ramírez de Cartagena^b, Gerard Arbat^b

5 ^aDepartment of Mathematics, Faculty of Sciences, University of Oviedo, 33007 Oviedo, Spain

6 ^bDepartment of Chemical and Agricultural Engineering and Technology, University of Girona, 17003
7 Girona, Catalonia, Spain

9 Abstract

10 Sand media filters are a key component of micro-irrigation systems since they help
11 preventing emitter clogging, which greatly affects the system performance. Dissolved
12 oxygen is an irrigation water quality parameter related to organic matter loading. Low
13 values of dissolved oxygen can cause crop root hypoxia and, therefore, agronomic
14 problems. Thus, an accurate prediction of dissolved oxygen values could be of great
15 interest, especially if effluents are used in micro-irrigation systems. The aim of this
16 study was to obtain a predictive model able to forecast the dissolved oxygen values at
17 the outlets of sand media filters. In this study, a Gaussian process regression (GPR)
18 model was used for predicting the output dissolved oxygen (DO_o) from data
19 corresponding to 547 filtration cycles of different sand filters using reclaimed effluent.
20 This optimisation technique involves kernel parameter setting in the GPR training
21 procedure, which significantly influences the regression accuracy. To this end, the
22 height of the filter bed, filtration velocity and filter inlet values of the electrical
23 conductivity, dissolved oxygen, pH, turbidity and water temperature were monitored

*Corresponding author. Tel.: +34-985103417; fax: +34-985103354.
E-mail address: lato@orion.ciencias.uniovi.es (P.J. García-Nieto).

24 and analysed. The significance of each variable on filtration performance is presented
25 and a model for forecasting the outlet dissolved oxygen obtained. Regression with
26 optimal hyperparameters was performed and a coefficient of determination of 0.90 for
27 DO_o was obtained when this new predictive GPR-based model was applied to the
28 experimental dataset. Agreement between experimental data and the model confirmed
29 the good performance of the latter.

30

31 *Keywords:* Gaussian process regression; Bayesian statistics; Machine learning
32 techniques; Drip irrigation; Clogging; Effluents

33

34 **Nomenclature**

35 Abbreviations

ANN	Artificial neural network
DE	Differential evolution
DO	Dissolved oxygen
GPR	Gaussian process regression
GEP	Gene expression programming
R^2	Coefficient of determination
RBF	Radial basis function
SCADA	Supervisory control and data acquisition
SE	Squared-exponential
SVM	Support vector machine
v	Filtration velocity, m h^{-1}
Symbols	
DO_i	Dissolved oxygen at filter inlet, mg l^{-1}

DO_o	Dissolved oxygen at filter outlet, mg l ⁻¹
δ_{ij}	Kronecker delta function
ε	Additive white noise
ℓ	Length-scale for the RBF kernel
σ_f^2	Variance for the RBF kernel
σ_n^2	Gaussian noise variance

36

37 **1. Introduction**

38 The substitution of conventional irrigation water by reclaimed effluents in areas of low
39 water availability is a common management strategy despite of its potential pollution
40 and health hazards (Ait-Mouheb et al., 2018). Among the different irrigation techniques
41 used, micro-irrigation shows several environmental and health advantages related
42 mainly to the reduced effluent exposure to humans and plants. However, one of the
43 most important disadvantages of applying effluents with micro-irrigation is emitter
44 clogging which can cause irrigation nonuniformity and system failure (Trooien & Hills,
45 2007). In order to avoid emitter clogging, micro-irrigation systems require effective
46 filtration (Nakayama, Boman, & Pitts, 2007) and sand media filters are the standard for
47 the protection of micro-irrigation systems using effluents (Trooien & Hills, 2017).

48

49 The level of dissolved oxygen (DO) decreases with the increased organic matter,
50 commonly present in wastewaters. So, DO, which can be determined easier and quicker
51 using sensors, is an indicator of irrigation water quality. Low DO values in the irrigation
52 water cause root oxygen deficiency, leading to low yields (Bhattarai, Midmore, &
53 Pendergast, 2008) and low quality (Zhou, Zhou, Xu, Muhammad, & Li, 2019). Usually,

54 DO increases through micro-irrigation systems, especially when water is released by the
55 emitters (Maestre–Valero & Martínez-Álvarez, 2010). The DO increase is slight in sand
56 media filters but it is considerably affected by the filter performance (Elbana, Ramírez
57 de Cartagena, & Puig-Bargués, 2012; Solé–Torres, Puig–Bargués, Duran–Ros, Arbat,
58 Pujol, & Ramírez de Cartagena, 2019b). Thus, the development of accurate models for
59 forecasting DO at filter outlets can be very useful for the appropriate management of
60 both sand filter performance and irrigation water quality. Optimal efficiency of drip
61 irrigation systems is required for implementing smart irrigation techniques which aim to
62 provide optimum use of the water resources (Canales-Ide, Zubelzu & Rodríguez-
63 Sinobas, 2019).

64

65 In this regard, advanced techniques such as artificial neural networks (ANN) (Puig–
66 Bargués, Duran-Ros, Arbat, Barragán, & Ramírez de Cartagena, 2012), gene expression
67 programming (GEP) (Martí et al., 2013) and support vector machines (SVM) (García–
68 Nieto, García–Gonzalo, Arbat, Duran–Ros, Ramírez de Cartagena, & Puig–Bargués,
69 2016) have been used for predicting the filtered volume and the value of dissolved
70 oxygen at sand media filter outlets. Recently, other machine learning techniques such as
71 gradient boosted regression have been applied to different aspects of the filter operation
72 (García–Nieto et al. 2017, 2018).

73

74 Thus, the application of an innovative methodology that combines a Gaussian process
75 regression (GPR) approach (Rasmussen, 2003; Kuhn & Johnson, 2018; Ebdén, 2015)
76 with a metaheuristic optimisation algorithm Differential Evolution (DE) (Storn & Price,
77 1997; Price, Storn, & Lampinen, 2005; Feoktistov, 2006; Chakraborty, 2008; Simon,

78 2013) to foretell the outlet dissolved oxygen in sand media filters used in
79 microirrigation systems could be an interesting approach since this issue has not yet
80 been yet addressed in previous investigations. GPR is a machine learning method
81 developed on the basis of statistical and Bayesian theory. As a nonparametric regression
82 method it can be considered a complex model with capability to model nonlinearities
83 and variable interactions (Rasmussen, 2003; Ebden, 2015). When GPR is compared
84 with other machine learning techniques, it has several advantages (Rasmussen &
85 Williams, 2006): (1) it has an important generalisation capacity; (2) the hyperparameters
86 in GPR can be self-adaptively calculated; and (3) the GPR outputs have clear
87 probabilistic meaning. In this study, the DE method is applied to optimise the GPR
88 hyperparameters. Previous researches show that GPR is an effective tool in many fields,
89 such as irrigation mapping (Chen, Lu, Luo, Pokhrel, Deb, Huang, & Ran, 2018), wind
90 engineering and industrial aerodynamics (Ma, Xu, & Chen, 2019), applied geophysics
91 (Noori, Hassani, Javaherian, Amindavar, & Torabi, 2019), applied demography (Wu &
92 Wang, 2018), psychology (Schulz, Speekenbrink, & Krause, 2018), mechanical
93 engineering (Kong, Chen, & Li, 2018), environmental engineering (Liu, Yang, Huang,
94 Wang, & Yoo, 2018), tracking and positioning (Ko, Klein, Fox, & Haehnelt, 2007a),
95 deformation observation (Rogers & Girolami, 2016), system identification and control
96 (Ko, Klein, Fox, & Haehnelt, 2007b) and so on. However, it has not been used for
97 predicting micro-irrigation sand filter performance.

98

99 The main objective of the this study was to predict the outlet dissolved oxygen (DO_o) in
100 sand media filters operating with reclaimed effluents by using Gaussian processes (GPs)
101 in combination with the DE parameter optimisation technique.

102 The structure of this paper is organised as follows: section 2 introduces the experimental
103 setup and variables involved in this study as well as the GPR method; section 3
104 describes the results obtained with this model by comparing the GPR results with the
105 experimental measurements, including the importance of the input variables and
106 validating the efficacy of the proposed approach; and finally, section 4 concludes this
107 study with a list of main findings.

108

109 **2. Materials and methods**

110 *2.1. Experimental setup*

111 The experimental setup was composed of 3 media filters fed with the reclaimed effluent
112 from the wastewater treatment plant of Celrà (Girona, Spain). Each filter had a different
113 underdrain design: inserted domes (model FA-F2-188, Regaber, Parets del Vallès,
114 Spain), arm collector (model FA1M, Lama, Gelves, Spain) and porous media (prototype
115 designed by Bové et al. (2017) (see Fig. 1).

116

117 Silica sand CA-07MS (Sibelco Minerales SA, Bilbao, Spain) with an effective diameter
118 (D_e , size opening which will pass 10% of the sand) of 0.48 mm and a coefficient of
119 uniformity (ratio of the sizes opening which will pass 60% and 10% of the sand
120 through, respectively) of 1.73 was used as filtration media in the three filters. Media
121 heights of 200 and 300 mm, were tested for each filter.

122

123 Each of the three filters operated alone for 8 h per day each. Nominal filtration
124 velocities 30 and 60 m h⁻¹ were tested in each filter. Each combination of media height
125 and filtration velocity was tested during 250 h. The filters were automatically

126 backwashed when the pressure loss across them reached 50 kPa for more than 1 min.
127 The backwashing was carried out for 3 min with previously filtered effluent that was
128 chlorinated for achieving 4 ppm target chlorine concentration.

129

130 Filtered and backwashed effluent volumes, pressures across the filter and some effluent
131 quality parameters before (pH, temperature, electrical conductivity, DO and turbidity)
132 and after (only DO and turbidity) being filtered were measured and recorded every
133 minute in a supervisory control and data acquisition system (SCADA) fully described
134 by Solé-Torres et al. (2019a). Once the experiment started, the performance of the
135 effluent quality sensors was assessed periodically by comparing its measurements with
136 results obtained by manual sampling and, if necessary, they were calibrated following
137 manufacturer recommendations.

138

139 **Fig. 1** - Picture of the experimental set-up with the three filter designs: (a) red: arm
140 collector; (b) blue: inserted domes; and (c) green: porous media prototype.

141

142 *2.2. Variables involved in the model and materials tested*

143 The main objective of this study was to compute the outlet dissolved oxygen as a
144 function of different experimentally measured parameters that the GPR-based model
145 needs as input. The output variable was the outlet dissolved oxygen (DO_o), which is an
146 indicator of the quality of the filtered effluent and it is directly related to the organic
147 load and the hypoxic risk of irrigation water.

148

149 The new predictive model used eight different operating variables commonly used for
150 characterising sand media filter performance as input variables (see Table 1) (Puig-
151 Bargués et al., 2012). After removing samples with missing data from the initial 637
152 samples, 547 satisfactory samples were obtained.

153

154 **Table 1** - Set of operation physical input variables used in this study and their names
155 along with their mean and standard deviation.

156

157 The operating input variables are as follows:

- 158 • Filter: three filter designs (porous, dome and arm collector underdrains) as
159 described in section 2.1. This is a categorical variable.
- 160 • Height of the filter bed (mm): an operating variable for sand filters. Two
161 different filter bed heights of 200 and 300 mm were tested for each filter.
- 162 • Filtration velocity (m h^{-1}): a operating variable related to filter operation. Two
163 filtration velocities (30 and 60 m h^{-1}) were tested for each filter since these
164 follow within the common range of velocities suggested by the manufacturers.
- 165 • Electrical conductivity ($\mu\text{S cm}^{-1}$): a general measure of water quality related to
166 salinity, which is a constraint in microirrigation (Tal, 2016).
- 167 • Dissolved oxygen (mg l^{-1}): a variable related to the ability of water to support
168 aerobic processes. This is a common parameter used for both controlling the
169 biological treatment in wastewater plants and measuring irrigation water quality.
- 170 • pH: a measure of water acidity or alkalinity.

- 171 • Water temperature (°C): temperature of the effluent at the filter inlet.
- 172 • Input turbidity (FNU): a key parameter for water quality that measures water
173 clarity, which depends on suspended solid load.
- 174 • Filtered volume (m³): a measure of the volume of effluent filtered in each
175 filtration cycle.

176

177 2.3. Gaussian process regression (GPR)

178 GPRs are Bayesian state-of-the-art tools for discriminative machine learning (i.e.,
179 regression, classification, and dimensionality reduction). GPs assume that a GP prior
180 governs the possible unobserved latent functions and the marginal likelihood of the
181 latent function. Thus, a priori observations shape this to produce posteriori probabilistic
182 estimates. Consequently, the joint distribution of training and test data is a
183 multidimensional GP, and the predicted distribution is estimated by conditioning based
184 on training data (Camps–Valls, 2016; Witten, Frank, Hall, & Pal, 2016).

185

186 To fix ideas, a Gaussian distribution is a probability distribution that explains the
187 random variables including vectors and scalars. On the one hand, this kind of
188 distribution is stated exactly through its mean and covariance: $x \sim N(\mu, \sigma^2)$. On the
189 other hand, a GP can be seen as a generalisation of the Gaussian probability distribution
190 and it applies over functions. From the functional space point of view, a GP is an
191 ensemble of random variables, that is to say, any finite number having a joint Gaussian
192 distribution.

193

194 2.3.1. *The fundamentals of GPR*

195 Let us assume that $D = \{(\mathbf{x}_i, y_i) / i = 1, 2, \dots, N\}$ depicts the training dataset of the
 196 Gaussian approach and the feature vectors $\mathbf{x}_i \in \mathcal{R}^n$ comprises the extracted features or
 197 the merged features and the pertinent segregation parameters. The observed target
 198 values y_i reproduce the outlet dissolved oxygen measured in a filtration process,
 199 respectively. $X = \{\mathbf{x}_i\}_{i=1}^N$ depicts the input matrix of training dataset,
 200 $\mathbf{y} = \{y_i\}_{i=1}^N$ symbolises the output vector. A GP $f(\mathbf{x})$ defines a priori over functions,
 201 which can be converted into a posteriori over functions once some data is obtained. A
 202 GP can be fully stated exactly by using its mean function $m(\mathbf{x})$ and covariance function
 203 $k(\mathbf{x}, \mathbf{x}')$. In this way, the Gaussian process is indicated as (Rasmussen & Williams,
 204 2006; Marsland, 2014; Witten, Frank, Hall, & Pal, 2016):

$$f(\mathbf{x}) \sim GP(m(\mathbf{x}), k(\mathbf{x}, \mathbf{x}')) \quad (1)$$

205 so that

$$\begin{aligned} m(\mathbf{x}) &= E[f(\mathbf{x})] \\ k(\mathbf{x}, \mathbf{x}') &= E\left[(f(\mathbf{x}) - m(\mathbf{x}))(f(\mathbf{x}') - m(\mathbf{x}'))^T\right] \end{aligned} \quad (2)$$

206 The mean function $m(\mathbf{x})$ depicts the anticipated value of the function $f(\mathbf{x})$ at the input
 207 point \mathbf{x} . The covariance function $k(\mathbf{x}, \mathbf{x}')$ can be taken into account as a measurement
 208 of the confidence level for $m(\mathbf{x})$, and it is required that $k(\cdot, \cdot)$ be a positive definite
 209 kernel. In general, the mean function is set to be zero for notation simplicity, but this is
 210 also reasonable if there is no a priori knowledge about the mean variable, as is the case
 211 in this study.

212 The choice of the covariance function is critical for the GP. It describes the assumptions
 213 about the latent regression model and, therefore, is also referred to as the prior
 214 (Schneider & Ertel, 2010). In this research, the affine mean function and squared-
 215 exponential (SE) covariance function are expressed as follows (Shi & Choi, 2011;
 216 Witten, Frank, Hall, & Pal, 2016; Kuhn & Johnson, 2018):

$$k_{\text{SE}}(\mathbf{x}, \mathbf{x}') = \sigma_f^2 \exp\left(-\frac{\|\mathbf{x} - \mathbf{x}'\|^2}{2l^2}\right) \quad (3)$$

217 being l the characteristic length-scale and σ_f^2 the signal variance. The parameter
 218 selection of the SE covariance function has a direct effect on the performance of the GP.
 219 Here, l controls the horizontal scale over which the function changes, and σ_f^2 controls
 220 the vertical scale of the function.

221

222 The function values $f(\mathbf{x})$ are not achievable in most applications. In practice, only the
 223 noisy observations are available and they are given by:

$$\mathbf{y} = f(\mathbf{x}) + \varepsilon \quad (4)$$

224 so that ε is the additive white noise. Besides, suppose that Gaussian noise is
 225 independent and identically distributed such that $\varepsilon \sim N(0, \sigma_n^2)$, where σ_n is the
 226 standard deviation of this noise. Any finite number of the observed values can also
 227 constitute an individual Gaussian process as given by (Witten, Frank, Hall, & Pal, 2016;
 228 Vidales, 2019):

$$\mathbf{y} \sim GP\left(m(\mathbf{x}), k(\mathbf{x}, \mathbf{x}') + \sigma_n^2 \delta_{ij}\right) = GP\left(0, k(\mathbf{x}, \mathbf{x}') + \sigma_n^2 \delta_{ij}\right) \quad (5)$$

229 where δ_{ij} is the Kronecker delta function described as:

230
$$\delta_{ij} = \begin{cases} 1 & \text{if } i = j \\ 0 & \text{otherwise} \end{cases}$$

231 The purpose of the GPR model is to foretell the function value \bar{f}^* and its variance
 232 $\text{cov}(f^*)$ given the new test point \mathbf{x}^* . In this sense, X^* depicts the input matrix of test
 233 dataset and N^* the size of test dataset. Taking into account the definition of GP, the
 234 observed values and the function values at new test points obey a joint Gaussian
 235 previous distribution which can be expressed as:

$$\begin{bmatrix} \mathbf{y} \\ \mathbf{f}^* \end{bmatrix} \sim N \left(\mathbf{0}, \begin{bmatrix} K(X, X) + \sigma_n^2 I & K(X, X^*) \\ K(X^*, X) & K(X^*, X^*) \end{bmatrix} \right) \quad (6)$$

236 where:

- 237 • $K(X, X)$: is the covariance matrix of training dataset;
- 238 • $K(X^*, X^*)$: is the covariance matrix of test dataset;
- 239 • $K(X, X^*)$: depicts the covariance matrix obtained from the training and test
 240 dataset. Furthermore $K(X^*, X) = K(X, X^*)^T$.

241 Since \mathbf{y} and \mathbf{f}^* are jointly distributed, it is possible to condition the prior on the
 242 observations (6) and determine how likely are predictions for \mathbf{f}^* . This can be expressed
 243 as:

$$\mathbf{f}^* | X^*, X, \mathbf{y} \sim N(\bar{\mathbf{f}}^*, \text{cov}(\mathbf{f}^*)) \quad (7)$$

244 where

$$\bar{\mathbf{f}}^* = E[\mathbf{f}^* | X^*, X, \mathbf{y}] = K(X^*, X) [K(X, X) + \sigma_n^2 I]^{-1} \mathbf{y} \quad (8)$$

$$\text{cov}(\mathbf{f}^*) = K(X^*, X^*) - K(X^*, X) [K(X, X) + \sigma_n^2 I]^{-1} K(X, X^*) \quad (9)$$

245 The subsequent distribution can be used for the forecast of new test input points.
 246 Indeed, $\bar{\mathbf{f}}^*$ is the predicted output value of the GPR model for test point. Additionally,
 247 confidence interval (CI) of the predicted output value can be calculated through the
 248 variance $\text{cov}(\mathbf{f}^*)$. For instance, the 95% CI can be determined by
 249 $\left[\bar{\mathbf{f}}^* - 2 \times \sqrt{\text{cov}(\mathbf{f}^*)}, \bar{\mathbf{f}}^* + 2 \times \sqrt{\text{cov}(\mathbf{f}^*)} \right]$. As a consequence, the GPR model not only
 250 supplies the predicted values but also furnishes the confidence level of the predicted
 251 results.

252

253 Finally, the GPR model is a nonparametric model since the predicted outputs rely only
 254 on the inputs and the observed values \mathbf{y} . In this way, parameters $\Theta = \{l, \sigma_f, \sigma_n\}$ are
 255 termed the hyperparameters of the GPR model.

256

257 2.3.2. Hyperparameter estimation

258 In order to carry out this study, the dataset was divided into a training set with 80% of
 259 the data, and a testing set with the remainder 20% of the data. A model was constructed
 260 and optimised with the training data. It was then tested with the test dataset and the
 261 optimisation of the parameters was performed with the help of the differential evolution
 262 (DE) technique.

263

264 The predictive performance of GPR model depends exclusively on the suitability of the
 265 chosen kernel. To estimate the kernel hyperparameters, an exhaustive search over a

266 discrete grid of values can be used, but this can be quite slow. The most usual method
 267 considers an empirical Bayes approach that maximises the marginal likelihood. That is,
 268 the optimal hyperparameters are achieved by maximising the log marginal likelihood.

269 The marginal likelihood $P(\mathbf{y}|X)$ is obtained, using Bayes' rule, as:

$$P(\mathbf{y}|X) = \int P(\mathbf{y}|f, X)P(f|X)df \quad (10)$$

270 The term marginal likelihood refers to the marginalisation over the function values \mathbf{f} .
 271 Since $\mathbf{y} \sim \mathcal{N}[0, K(X, X)]$, the log marginal likelihood can be written as:

$$\log p(\mathbf{y}|\hat{\mathbf{u}}X) = -\frac{1}{2}\mathbf{y}K_y^{-1}\mathbf{y} - \frac{1}{2}\log \hat{\mathbf{u}}K_y\hat{\mathbf{u}} - \frac{N}{2}\log(2\pi) \quad (11)$$

272 where $K_y = K + \sigma_n^2 I$, $K = K(X, X)$ and $\hat{\mathbf{u}}$ is the determinant. In this expression, the
 273 first term is a data-fit term, the second term (always positive), and subtracted from it, is
 274 a model complexity penalty, and the last term is simply a normalisation constant. This
 275 expression therefore shows that the criterion of maximum marginal likelihood avoids
 276 the problem of over-fitting because if two models are explaining the observed data with
 277 the simplest one being chosen (Murphy, 2012; Witten, Frank, Hall, & Pal, 2016).

278

279 Following parameter initialisation, the optimal hyperparameters
 280 $\Theta' = \arg \max_{\Theta} \log p(\mathbf{y}|X, \Theta)$ can be calculated using any standard evolutionary
 281 optimiser. In this study, the metaheuristic optimisation algorithm, denominated the DE
 282 algorithm (Storn & Price, 1997; Price, Storn, & Lampinen, 2005; Feoktistov, 2006;
 283 Simon, 2013), was used. The process is shown in Fig. 2.

284

285 **Fig. 2** – GPR Model selection using the DE optimisation technique.

286 2.4. The goodness-of-fit of this approach

287 Eight predicting variables were used (see section 2.2) to construct the new GPR-based
288 model. The output predicted variable was the outlet dissolved oxygen. To predict the
289 outlet dissolved oxygen from other input operating parameters, it is necessary to choose
290 the model that best fits the experimental data. To determine the goodness-of-fit, the
291 criterion considered here was the coefficient of determination R^2 (Picard & Cook, 1984;
292 Freedman, Pisani, & Purves, 2007). A dataset takes values t_i , each of which has an
293 associated modelled value y_i . The former are usually termed the observed values and
294 the latter often referred to as the predicted values. The dataset variability is measured
295 through different sums of squares as follows (Freedman, Pisani, & Purves, 2007):

- 296 • $SS_{tot} = \sum_{i=1}^n (t_i - \bar{t})^2$: the total sum of squares, proportional to the sample variance.
- 297 • $SS_{reg} = \sum_{i=1}^n (y_i - \bar{t})^2$: the regression sum of squares, also termed the explained
298 sum of squares.
- 299 • $SS_{err} = \sum_{i=1}^n (t_i - y_i)^2$: the residual sum of squares.

300 Note that in the previous sums, \bar{t} is the mean of the n observed data:

$$\bar{t} = \frac{1}{n} \sum_{i=1}^n t_i \quad (12)$$

301 Taking into account the above sums, the coefficient of determination is defined via:

$$R^2 \equiv 1 - \frac{SS_{err}}{SS_{tot}} \quad (13)$$

302 Thus, a coefficient of determination value of 1.0 indicates that the regression curve fits
303 the data perfectly.

304

305 The value of R^2 was calculated using the optimised model with the testing dataset. The
306 module Gpy from the Gaussian process framework found in Python (Gpy, 2014;
307 Martin, 2018), along with the DE technique (Storn & Price, 1997; Price, Storn, &
308 Lampinen, 2005; Simon, 2013) were used to construct the final regression model.

309

310 It is well known that the GPR technique depends strongly on the following
311 hyperparameters (Friedman & Roosen, 1995; Aggarwal, 2015; Larose, 2015; Witten,
312 Frank, Hall, & Pal, 2016; Tan, Steinbach, Karpatne, & Kumar, 2018):

313 • Variance (σ_f^2):the signal variance that controls the vertical scale of the kernel
314 function.

315 • Lengthscale (ℓ):the characteristic length-scale that controls the horizontal scale
316 over which the kernel function changes.

317 • Gaussian noise variance (σ_n^2): if ε is the additive white noise and the Gaussian
318 noise is independent and identically distributed such that $\varepsilon \sim N(0, \sigma_n^2)$, then σ_n^2
319 is the variance of this noise.

320 1. A novel GPR-based model was constructed selecting as the dependent variable
321 the outlet dissolved oxygen from the other eight remaining variables which were
322 designated as input variables in the granular filters (Tien, 2012; Bové, Arbat,

323 Duran–Ros, Pujol, Velayos, Ramírez de Cartagena, & Puig–Bargués, 2015) and
324 studying their effect in order to optimise calculation by analysing R^2 .

325

326 As previously mentioned, this GPR technique is greatly dependent on the
327 hyperparameters: variance (σ^2); lengthscale (ℓ) and the Gaussian noise variance (σ_n^2).

328 The traditional way of performing hyperparameter optimisation has been *grid search*, or
329 a *parameter sweep*, which is simply an exhaustive searching through a manually
330 specified subset of the hyperparameter space of a learning algorithm. In this study, the
331 metaheuristic optimisation algorithm, the DE algorithm (Storn & Price, 1997; Price,
332 Storn, & Lampinen, 2005; Feoktistov, 2006; Simon, 2013) was used for
333 multidimensional real-valued functions but it did not use the gradient of the problem
334 being optimised, thus the DE did not require the optimisation problem to be
335 differentiable, as is required by classic optimisation methods such as the gradient
336 descent and quasi-Newton methods. Like other algorithms in this evolutionary category,
337 the DE maintains a population of candidate solutions, which are recombined and
338 mutated to produce new individuals which are chosen according to the value of their
339 performance function (Storn & Price, 1997). What characterises DE is the use of test
340 vectors, which compete with individuals in the current population in order to survive.

341

342 Additionally, the importance of the variables was studied. As categorical variables are
343 present, the chosen method depends on removing a variable, evaluating the new model
344 performance and comparing it with the performance of the full model. The greater the
345 decrease in the goodness-of-fit parameter, the greater the importance of the removed
346 independent variable.

347 3. Results and discussion

348 As stated earlier, the outlet dissolved oxygen was used as output dependent variable of
349 the proposed GPR-based model. The prediction performed from the independent
350 variables (Tien, 2012) was satisfactory.

351 Table 2 shows the optimal hyperparameters of the best fitted GPR-based model found
352 with the DE technique. The objective function value, in this case the marginal
353 likelihood was optimised to a value of 239 using the DE technique using the training
354 set.

355

356 **Table 2** - Optimal hyperparameters of the best fitted GPR-based model found with the
357 DE technique: variance σ_f^2 and lengthscale ℓ for the RBF kernel, the Gaussian noise
358 variance σ_n^2 for the optimised models for the training set.

359

360 Taking into account the results achieved, the GPR technique in combination with the
361 DE meta-heuristic optimisation method was able to build models with a high
362 performance for estimating the outlet dissolved oxygen in micro-irrigation sand filters
363 fed with effluents using the test set. Indeed, the coefficient of determination (R^2) of the
364 fitted GPR model was of 0.9023 with a correlation coefficient of 0.9499 for the outlet
365 dissolved oxygen.

366

367 A graphical representation of the terms that formed the best fitted GPR-based model for
368 the outlet dissolved oxygen (DO_o) is shown below in Figs. 3 and 4. The first order
369 terms, that is, the variations of the dependent variable when all the variables but one are

370 constant (its median value) is shown in Fig 3. The graphs suggest that the variable DO_i
371 is the main influence for the variations in DO_i , while other variables as pH and
372 temperature do not significantly affect this variable as these curves are almost constant.
373 The same effect can be shown in the surfaces that represent the second order
374 relationships, that is, leaving all the independent variables constant but two. Again, it
375 can be seen that the main influence in rapid change of output variable was due to the
376 DO_i .

377

378 **Fig. 3** - First-order terms for some of the independent variables for the dependent
379 variable output dissolved oxygen (DO_o).

380

381 **Fig. 4** - Second-order terms of some of the independent variables for the dependent
382 variable output dissolved oxygen (DO_o).

383

384 The significance rankings for the input variables predicting the outlet dissolved oxygen
385 (output variable) in this complex nonlinear study are shown in Table 3 and Fig. 5. As
386 there are some categorical variables such as the filter type involved, the method where
387 discarding one independent variable from the model at a time and taking into account
388 the decrease in goodness-of-fit, in this case, the marginal likelihoods, is shown in Table
389 3. The result is, that for the GPR model, the most significant variable in DO_o prediction
390 is the DO_i , followed by (in order) the type of filter, water temperature, height of the
391 filter bed, pH, velocity, turbidity, and electrical conductivity.

392

393 **Table 3** - Log marginal likelihood variation value between the full model and the model
394 without the variable for the outlet dissolved oxygen (DO_o) model.

395

396 **Fig. 5** - Relative relevance of the variables in the GPR model for the outlet dissolved
397 oxygen (DO_o).

398

399 As it could be anticipated, DO_o was highly dependent on DO_i since organic pollutants
400 are retained across filter media and chlorination of filter backwashing water reduced
401 microorganisms level, and therefore less oxygen is consumed and dissolved oxygen
402 could increase. However, DO removal depended also on media particle size (Elbana,
403 Ramírez de Cartagena, & Puig-Bargués, 2012) and on the interaction between filter type
404 and filtration velocity, considering input inlet DO as a co-variable (Solé-Torres, Puig-
405 Bargués, Duran-Ros, Arbat, Pujol, & Ramírez de Cartagena, 2019b). The filter type had
406 also a contribution on the results since different underdrain designs affect backwashing
407 performance and frequency (Burt, 2010), which is directly related to DO removal
408 (Enciso-Medina, Multer, & Lamm, 2011; Elbana, Ramírez de Cartagena, & Puig-
409 Bargués, 2012). The third parameter is temperature, but this is also logical since DO
410 values are temperature dependent.

411

412 The importance of DO_i for estimating DO_o has been previously observed by Martí et al.
413 (2013) and García-Nieto et al. (2016), working with different types of models. Martí et
414 al. (2013) observed that pH, EC and pressure loss, but not temperature, García-Nieto et
415 al. (2016) found that inlet turbidity and pressure loss were also considered as influential

416 parameters for predicting DO_o . Thus, the results highlight the importance of correctly
417 assessing the performance of each prediction model.

418

419 In conclusion, this research was able to estimate the outlet dissolved oxygen (output
420 variable) in agreement with the actual experimental values observed using the GPR–
421 based model with accuracy as well as success. Indeed, Fig. 6 shows the comparison
422 among the DO_o values observed and those predicted by using the GPR model with the
423 testing set. The values predicted by the model using the samples of the testing dataset
424 show a very good agreement with the observed values. As it can be seen, predicted
425 values are very close to the observed values or within the 95% confidence interval. This
426 is to be expected since the coefficient of determination was equal to 0.90. Therefore, in
427 order to achieve the best effective approach in this regression problem it is mandatory
428 the use of a GPR model with a DE optimisation technique.

429

430 **Fig. 6** - Observed and predicted DO_o values, taking into account the confidence interval,
431 by using the GPR–based model with the testing set ($R^2 = 0.9023$).

432

433 **4. Conclusions**

434 Taking into account the experimental observations and numerical predictions, the main
435 findings of this study can be summarised as follows:

- 436 • Firstly, the development of novel data-driven diagnostic techniques is very
437 useful to predict the DO_o from the experimental measurements. In this sense, the

438 new GPR-based method used here is useful to evaluate the outlet dissolved
439 oxygen in sand media filters used in microirrigation systems.

440 • Secondly, the assumption that the outlet dissolved oxygen diagnosis can be
441 accurately modelled by using a hybrid GPR-based model in granular filters was
442 confirmed.

443 • Thirdly, a reasonable coefficient of determination (0.9023) was obtained when
444 this GPR-based model was applied to the experimental dataset corresponding to
445 the DO_o .

446 • Fourthly, the significance order of the input variables involved in the prediction
447 of the outlet dissolved oxygen in sand media filters was set. This is one of the
448 main findings in this work. Specifically, input variable dissolved oxygen (DO_i)
449 could be considered the most influential parameter in the prediction of the DO_o .
450 In this regard, it is also important to highlight the influential role of the type of
451 filter in the dependent variable outlet dissolved oxygen.

452 • Finally, the influence of the hyperparameters setting of the GPR approach on the
453 DO_o regression performance was set up.

454 In summary, this methodology could be applied to other filtration processes with similar
455 or distinct filter media types with success, but it is always necessary to take into account
456 the characteristics of each filter and experiment. Consequently, an effective GPR-based
457 model is a good practical solution to the problem of the determining DO_o in the sand
458 media filters usually used in microirrigation systems.

459

460

461 **Acknowledgements**

462 Authors wish to acknowledge the computational support provided by the Department of
463 Mathematics at University of Oviedo as well as financial support of the Spanish
464 Research Agency through grants AGL2015-63750-R and RTI2018-094798-B-100.
465 Additionally, we would like to thank Anthony Ashworth for his revision of English
466 grammar and spelling of the manuscript.

467

468 **References**

- 469 Aggarwal, C.C. (2015). *Data mining: the textbook*. New York, USA: Springer.
- 470 Ait-Mouheb, N., Bahri, A., Ben Thayer, B., Benyahia, B., Bourrié, G., Cherki, B. et al.
471 (2018). The reuse of reclaimed water for irrigation around the Mediterranean Rim: a
472 step towards a more virtuous cycle? *Regional Environmental Change*, 18, 693–705.
- 473 Bhattarai, S.P., Midmore, D.J. & Pendergast, L. (2008). Yield, water-use efficiencies
474 and root distribution of soybean, chickpea and pumpkin under different subsurface
475 drip irrigation depths and oxygenation treatments in vertisols. *Irrigation Science*,
476 26(5), 439–450.
- 477 Bové, J., Arbat, G., Duran–Ros, M., Pujol, T., Velayos, J., Ramírez de Cartagena, F., &
478 Puig–Bargués, J. (2015). Pressure drop across sand and recycled glass media used in
479 micro irrigation filters. *Biosystems Engineering*, 137, 55–63.
- 480 Bové, J., Puig–Bargués, J., Arbat, G., Duran–Ros, M., Pujol, T., Pujol, J., & Ramírez de
481 Cartagena, F. (2017). Development of a new underdrain for improving the
482 efficiency of microirrigation sand media filters. *Agricultural Water Management*,
483 179, 296–305.

484 Camps–Valls, G., Verrelst, J., Muñoz–Mari, J., Laparra, V., Mateo–Jimenez, F., &
485 Gomez–Dans, J. (2016). A survey on Gaussian processes for earth-observation data
486 analysis: a comprehensive investigation. *IEEE Geoscience and Remote Sensing*
487 *Magazine*, 4(2), 58–78.

488 Canales-Ide, F., Zubeizu, S., & Rodríguez-Sinobas, L. (2019). Irrigation systems in
489 smart cities coping with water scarcity: The case of Valdebebas, Madrid (Spain).
490 *Journal of Environmental Management*, 247, 187-195.

491 Chakraborty, U.K. (2008). *Advances in differential evolution*. Berlin: Springer.

492 Chen, Y., Lu, D., Luo, L., Pokhrel, Y., Deb, K., Huang, J., & Ran, Y. (2018). Detecting
493 irrigation extent, frequency, and timing in a heterogeneous arid agricultural region
494 using MODIS time series, Landsat imagery, and ancillary data. *Remote Sensing of*
495 *Environment*, 204, 197–211.

496 Ebden, M. (2015). Gaussian processes: a quick introduction.
497 <https://arxiv.org/pdf/1505.02965.pdf>.

498 Elbana, M., Ramírez de Cartagena, F., & Puig-Bargués, J. (2012). Effectiveness of sand
499 media filters for removing turbidity and recovering dissolved oxygen from a
500 reclaimed effluent used for micro-irrigation. *Agricultural Water Management*, 111,
501 27–33.

502 Enciso-Medina, J., Multer, W.L. & Lamm, F.R. (2011). Management, maintenance, and
503 water quality effects on the long-term performance of subsurface drip irrigation
504 systems. *Applied Engineering in Agriculture*, 27 (6), 969–978.

505 Feoktistov, V. (2006). *Differential evolution: in search of solutions*. New York:
506 Springer.

507 Freedman, D., Pisani, R., & Purves, R. (2007). *Statistics*. New York: W.W. Norton &
508 Company, New York.

509 García-Nieto, P.J., García-Gonzalo, E., Arbat, G., Duran-Ros, M., Ramírez de
510 Cartagena, F., & Puig-Bargués, J. (2016). A new predictive model for the filtered
511 volume and outlet parameters in micro-irrigation sand filters fed with effluents using
512 the hybrid PSO-SVM-based approach. *Computers and Electronics in Agriculture*,
513 125, 74–80.

514 García-Nieto, P.J., García-Gonzalo, E., Arbat, G., Duran-Ros, M., Ramírez de
515 Cartagena, F., & Puig-Bargués, J. (2018). Pressure drop modelling in sand filters in
516 micro-irrigation using gradient boosted regression trees. *Biosystems Engineering*,
517 171, 41–51.

518 García-Nieto, P.J., García-Gonzalo, E., Bové, J., Arbat, G., Duran-Ros, M., & Puig-
519 Bargués, J. (2017). Modeling pressure drop produced by different filtering media in
520 microirrigation sand filters using the hybrid ABC-MARS-based approach, MLP
521 neural network and M5 model tree. *Computers and Electronics in Agriculture*, 139,
522 65–74.

523 GPpy, 2014. A Gaussian process framework in python.
524 <http://github.com/SheffieldML/GPy>.

525 Ko, J., Klein, D.J., Fox, D., & Haehnel, D. (2007a). GP-UKF: Unscented Kalman
526 filters with Gaussian process prediction and observation models. In 2007 IEEE/RSJ
527 International Conference on Intelligent Robots and Systems (pp. 1901–1907). San
528 Diego, CA, USA: IEEE.

529 Ko, J., Klein, D.J., Fox, D., & Haehnel, D. (2007b). Gaussian processes and
530 reinforcement learning for identification and control of an autonomous blimp. In

531 Proceedings 2007 IEEE International Conference on Robotics and Automation (pp.
532 742–747). Roma, Italy: IEEE.

533 Kong, D., Chen, Y., & Li, N. (2018). Gaussian process regression for tool wear
534 prediction. *Mechanical Systems and Signal Processing*, 104, 556–574.

535 Kuhn, M., & Johnson, K. (2018). *Applied predictive modeling*. New York, USA:
536 Springer.

537 Larose, D.T. (2015). *Data mining and predictive analytics*. New York, USA: Wiley.

538 Liu, H., Yang, C., Huang, M., Wang, D., & Yoo, C. (2018). Modeling of subway indoor
539 air quality using Gaussian process regression. *Journal of Hazardous Materials*, 359,
540 266–273.

541 Ma, X., Xu, F., & Chen, B. (2019). Interpolation of wind pressures using Gaussian
542 process regression. *Journal of Wind Engineering & Industrial Aerodynamics*, 188,
543 30–42.

544 Maestre-Valero, J.F., & Martínez-Álvarez, V. (2010). Effects of drip irrigation systems
545 on the recovery of dissolved oxygen from hypoxic water. *Agricultural Water
546 Management*, 97, 1806–1812.

547 Marsland, S. (2014). *Machine learning: an algorithmic perspective*. Boca Raton, FL,
548 USA: Chapman and Hall/CRC Press.

549 Martí, P., Shiri, J., Duran-Ros, M., Arbat, G., Ramírez de Cartagena, F., & Puig-
550 Bargués, J. (2013). Artificial neural networks vs. Gene Expression Programming for
551 estimating outlet dissolved oxygen in micro-irrigation sand filters fed with effluents.
552 *Computers and Electronics in Agriculture*, 99, 176–185.

553 Martin, O. (2018). *Bayesian analysis with python*. Birmingham, UK: Packt Publishing.

- 554 Murphy, K.P. (2012). *Machine learning: a probabilistic perspective*. Cambridge, MA,
555 USA: The MIT Press.
- 556 Nakayama, F.S., Boman, B.J., & Pitts, D.J. (2007). Maintenance. In: Lamm, F.R.,
557 Ayars, J.E. & Nakayama, F.S. (Eds.), *Microirrigation for Crop Production. Design,*
558 *Operation, and Management* (pp. 389–430). Amsterdam, Netherlands: Elsevier.
- 559 Noori, M., Hassani, H., Javaherian, A., Amindavar, H., & Torabi, S. (2019). Automatic
560 fault detection in seismic data using Gaussian process regression. *Journal of Applied*
561 *Geophysics*, 163, 117–131.
- 562 Paananen, T., Piironen, J., Andersen, M.R., & Vehtari, A. (2019). Variable selection for
563 Gaussian processes via sensitivity analysis of the posterior predictive distribution. In
564 Proceedings of the 22nd International Conference on Artificial Intelligence and
565 Statistics (AISTATS), Proceedings of Machine Learning Research (PMLR) (pp.
566 1743–1752). Naha, Okinawa, Japan: arXiv:1712.08048 [stat.ME], Cornell
567 University, USA.
- 568 Picard, R., & Cook, D. (1984). Cross-validation of regression models. *Journal of the*
569 *American Statistical Association*, 79(387), 575–583.
- 570 Piironen, J., & Vehtari, A. (2016). Projection predictive model selection for Gaussian
571 processes. In 2016 IEEE 26th International Workshop on Machine Learning for
572 Signal Processing (MLSP) (pp. 1–6). Vietri sul Mare, Italy: IEEE.
- 573 Price, K., Storn, R.M., & Lampinen, J.A. (2005). *Differential evolution: A practical*
574 *approach to global optimization*. Berlin: Springer.
- 575 Puig–Bargués, J., Duran–Ros, M., Arbat, G., Barragán, J., & Ramírez de Cartagena, F.
576 (2012). Prediction by neural networks of filtered volume and outlet parameters in

577 micro-irrigation sand filters using effluents. *Biosystems Engineering*, 111(1), 126–
578 132.

579 Rasmussen, C.E. (2003). *Gaussian processes in machine learning: summer school on*
580 *machine learning*. Berlin, Germany: Springer.

581 Rasmussen, C.E., & Williams, C.K.I. (2006). *Gaussian processes for machine learning*.
582 Cambridge, MA, USA: The MIT Press.

583 Rogers, S., & Girolami, M. (2016). *A first course in machine learning*. Boca Raton, FL,
584 USA: Chapman and Hall/CRC.

585 Schneider, M., & Ertel, W. (2010). Robot learning by demonstration with local
586 Gaussian process regression. In: The 2010 IEEE/RSJ International Conference on
587 Intelligent Robots and Systems (pp. 255–260). Taipei, Taiwan: IEEE.

588 Schulz, E., Speekenbrink, M., & Krause, A. (2018). A tutorial on Gaussian process
589 regression: Modelling, exploring, and exploiting functions. *Journal of Mathematical*
590 *Psychology*, 85, 1–16.

591 Seeger, M. (2000). Bayesian model selection for support vector machines, Gaussian
592 processes and other kernel classifiers. In NIPS'99 Proceedings of the 12th
593 International Conference on Neural Information Processing Systems (vol. 12, pp.
594 603–609). Cambridge, MA, USA: The MIT Press.

595 Shi, J.Q., & Choi, T. (2011). *Gaussian process regression analysis for functional data*.
596 Boca Raton, FL, USA: Chapman and Hall/CRC Press.

597 Simon, D. (2013). *Evolutionary optimization algorithms*. New York: Wiley.

598 Solé–Torres, C., Duran–Ros, M., Arbat, G., Pujol, J., Ramírez de Cartagena F., & Puig–
599 Bargués, J. (2019a). Assessment of field water uniformity distribution in a
600 microirrigation system using a SCADA system. *Water*, 11(7), 1346–1359.

601 Solé–Torres, C., Puig–Bargués, J., Duran–Ros, M., Arbat, G., Pujol, J., & Ramírez de
602 Cartagena, F. (2019b). Effect of underdrain design, media height and filtration
603 velocity on the performance of microirrigation sand filters using reclaimed effluents.
604 *Biosystems Engineering*, 187, 292–304.

605 Storn, R., & Price, K. (1997). Differential evolution - a simple and efficient heuristic for
606 global optimization over continuous spaces. *Journal of Global Optimization*, 11,
607 341–359.

608 Tan, P.–N., Steinbach, M., Karpatne, A., Kumar, V. (2018). *Introduction to data*
609 *mining*. Oxford, UK: Pearson.

610 Tien, C. (2012). *Principles of filtration*. Kidlington, Oxford, UK: Elsevier.

611 Trooien, T.P., & Hills, D.J. (2007). Application of biological effluent. In Lamm, F.R.,
612 Ayars, J.E., & Nakayama, F.S. (Eds.), *Microirrigation for Crop Production. Design,*
613 *Operation and Management* (pp. 329–356). Amsterdam: Elsevier.

614 Vidales, A. (2019). *Machine learning with MATLAB: Gaussian process regression,*
615 *analysis of variance and Bayesian optimization*. Independently published.

616 Witten, I.H., Frank, E., Hall, M.A., Pal, C.J. (2016). *Data mining: practical machine*
617 *learning tools and techniques*. Cambridge, MA, USA: Morgan Kaufmann.

618 Wu, R., & Wang, B. (2018). Gaussian process regression method for forecasting of
619 mortality rates. *Neurocomputing*, 316, 232–239.

620 Zhou, Y., Zhou, B., Xu, F., Muhammad, T., Li, Y. (2019). Appropriate dissolved
621 oxygen concentration and application stage of micro-nano bubble water oxygenation
622 in greenhouse crop plantation. *Agricultural Water Management*, 223, 105713.

623



Fig. 1 - Picture of the experimental set-up with the three filter designs: (a) red: arm collector; (b) blue: inserted domes; and (c) green: a porous media prototype.

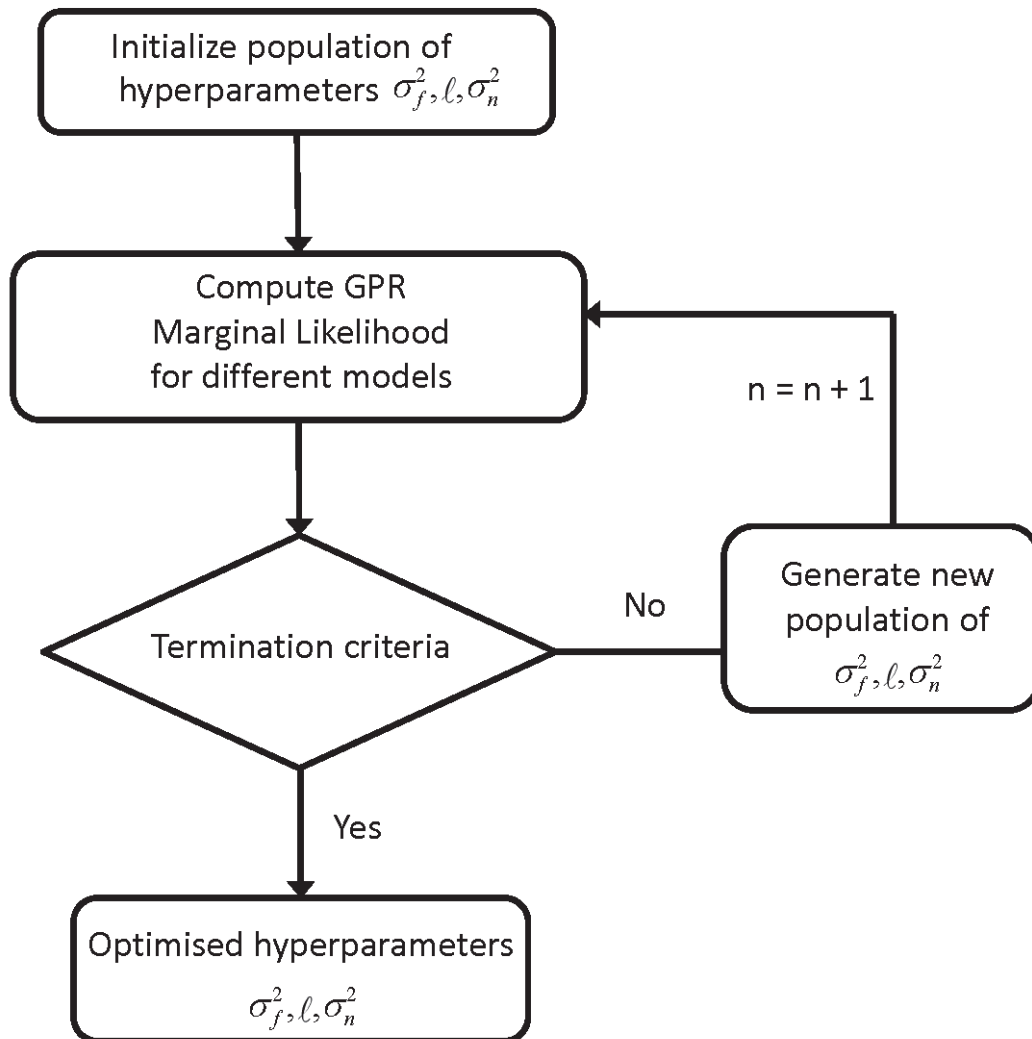


Fig. 2 – GPR Model selection using the DE optimisation technique.

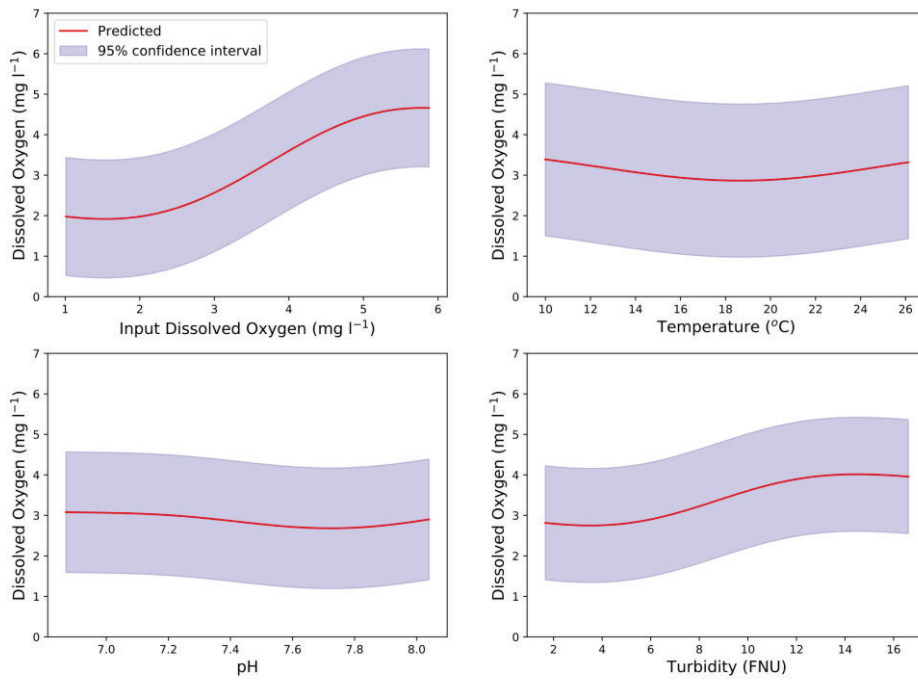


Fig. 3 - First-order terms for some of the independent variables for the dependent variable output dissolved oxygen (DO_o).

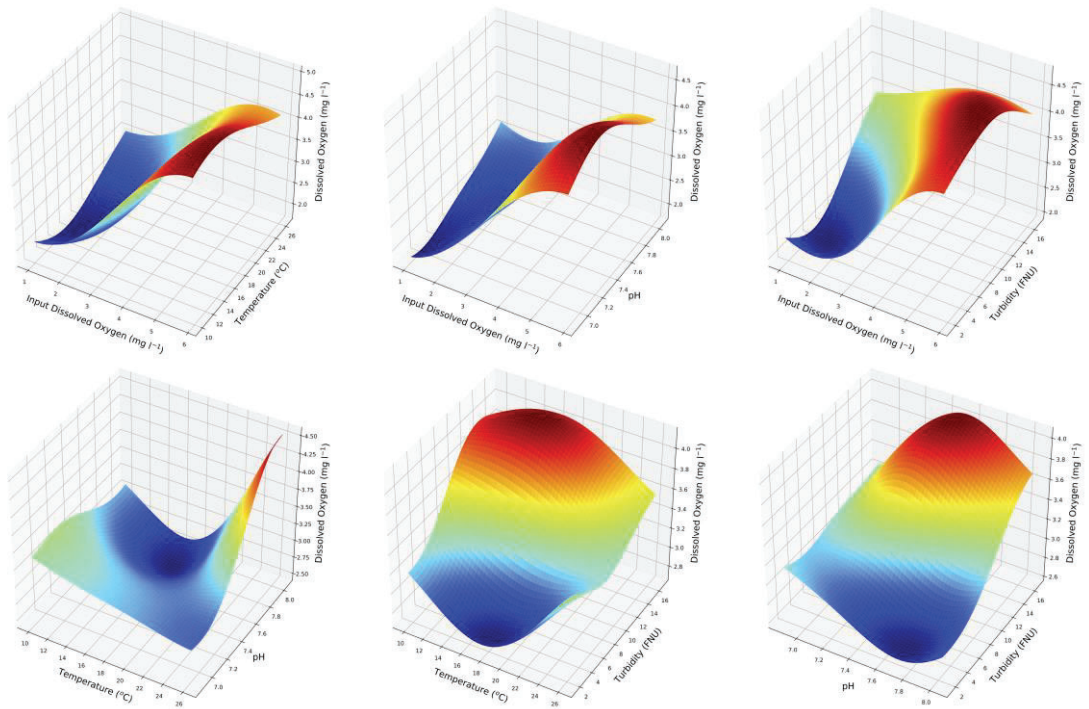


Fig. 4 - Second-order terms of some of the independent variables for the dependent variable output dissolved oxygen (DO_o).

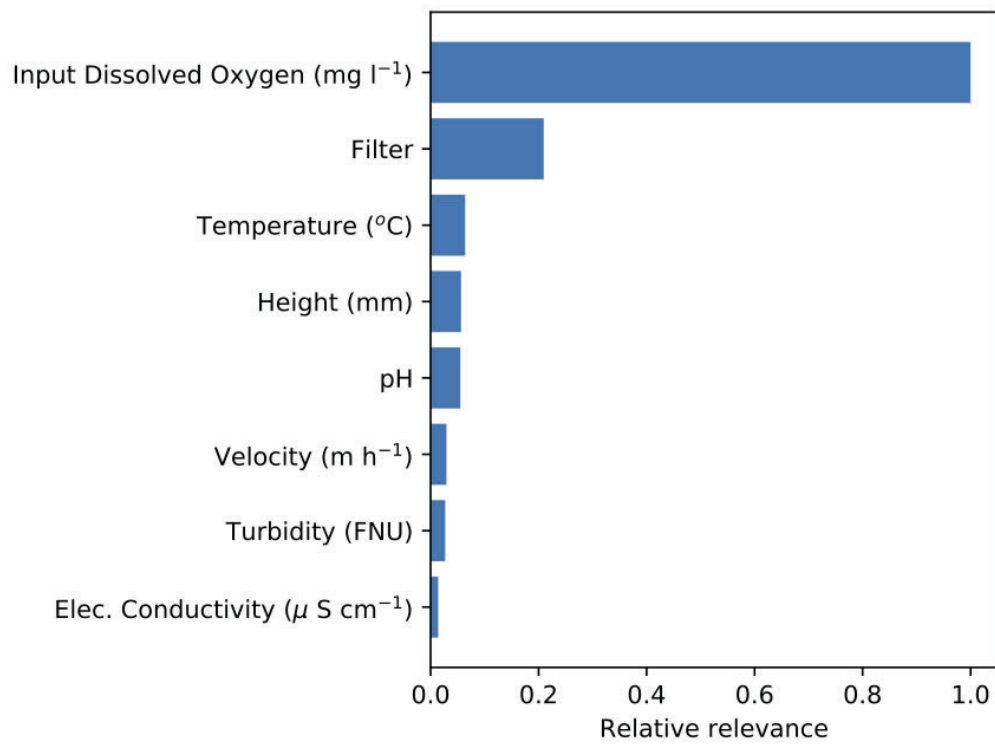


Fig. 5 - Relative relevance of the variables in the GPR model for the outlet dissolved oxygen (DO_o).

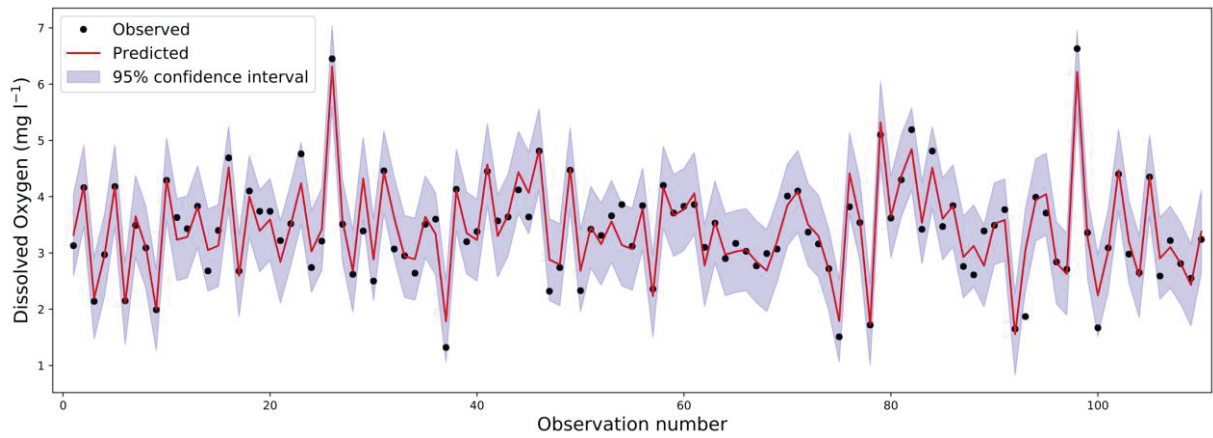


Fig. 6 - Observed and predicted DO_o values, taking into account the confidence interval, by using the GPR-based model with the testing set ($R^2 = 0.9023$).

Table 1 - Set of operation physical input variables used in this study and their names along with their means and standard deviations.

Input variables	Name of the variable	Mean	Standard deviation
Filter media type	Filter	--	--
Height of the filter bed (mm)	H	256.31	49.601
Filtration velocity (m h^{-1})	v	49.909	14.174
Electrical conductivity ($\mu\text{ S cm}^{-1}$)	CE_i	2575.6	497.68
Input dissolved oxygen (mg l^{-1})	DO_i	3.3529	0.9860
pH	pH_i	7.3526	0.2229
Input turbidity (FNU)	$Turb_i$	6.1029	2.5898
Water temperature ($^{\circ}\text{C}$)	T_i	20.002	3.3486

Table 2 - Optimal hyperparameters of the best fitted GPR-based model found with the DE technique: variance σ_f^2 and length-scale ℓ for the RBF kernel, the Gaussian noise variance σ_n^2 , and the corresponding objective function value for the optimized models for the training set.

Output variable	σ_f^2	ℓ	σ_n^2	Objective function value
DO_o	1.57	1.97	0.0636	239

Table 3 - Log marginal likelihood variation value between the full model and the model without the variable for the DO_o model.

Variable	Likelihood variation
Input dissolved Oxygen (mg l^{-1})	589.62
Filter	123.51
Water temperature ($^{\circ}\text{C}$)	37.77
Height (mm)	332.1
pH	32.45
Velocity (m h^{-1})	17.31
Input turbidity (FNU)	15.96
Electrical Conductivity ($\mu\text{S cm}^{-1}$)	8.25